

Published in final edited form as:

Chem Sci. 2010 September 1; 1(3): 387–392. doi:10.1039/C0SC00280A.

Stereoselectivity in Oxyallyl–Furan 4+3 Cycloadditions: Control of Intermediate Conformations and Dispersive Stabilisation with Evans' Oxazolidinones

Elizabeth H. Krenske^a, K. N. Houk^a, Andrew G. Lohse^b, Jennifer E. Antoline^b, and Richard P. Hsung^b

K. N. Houk: houk@chem.ucla.edu; Richard P. Hsung: rphsung@pharmacy.wisc.edu

^a Department of Chemistry and Biochemistry, University of California, Los Angeles, CA 90095, USA

^b Division of Pharmaceutical Sciences and Department of Chemistry, University of Wisconsin, Madison, WI 53705, USA

Abstract

Chiral oxazolidinones were previously thought to control cycloaddition stereoselectivity by steric crowding of one face of the substrate. We have discovered that in 4+3 cycloaddition reactions of oxyallyls, the stereoselection is caused instead by stabilising CH– π interactions that lead to reaction at the *more* crowded face of the oxazolidinone. Density functional theory calculations on the 4+3 cycloadditions of oxazolidinone-substituted oxyallyls with furans establish unexpected transition state conformations and a new explanation of selectivity.

Introduction

Amino acid-derived oxazolidinones are used extensively as chiral auxiliaries, following their introduction by Evans.¹ They have been applied to various cycloaddition reactions, including Diels–Alder^{2–4} and 1,3-dipolar⁵ cycloadditions. We have found that they also provide useful stereoselectivities in the (4 + 3) cycloadditions of dienes with oxyallyls. These (4 + 3) cycloadditions are a key step in the transformation shown in Scheme 1. Oxidation of an allenamide with DMDO generates an oxyallyl, which is then trapped with a furan.^{6,7} This sequence is a valuable synthetic procedure for formation of 7-membered carbocycles,^{8,9} which had previously been achieved using various other chiral, donor-substituted oxyallyl cations.^{10,11} Use of 4-phenyloxazolidinone as the auxiliary (R = Ph) provided the diastereomeric *endo* cycloadducts **I** and **II** in a ratio of 82:18,¹² and the ratio increased to $\geq 96:4$ when ZnCl₂ was included in the reaction mixture.⁶

The transformation shown in Scheme 1 is believed to involve the oxyallyl **1** (Scheme 2). The C _{α} –N bond in **1** is expected to have substantial double bond character, leading to the possibility of *E* and *Z* isomers.

The mechanism by which oxazolidinones control cycloaddition stereoselectivity was examined by Evans during studies of Diels–Alder reactions (Scheme 3). These reactions

© The Royal Society of Chemistry [year]

Correspondence to: K. N. Houk, houk@chem.ucla.edu; Richard P. Hsung, rphsung@pharmacy.wisc.edu.

† Electronic Supplementary Information (ESI) available: Details of the structural isomers of **1Ph** and higher-energy cycloaddition pathways; studies of solvation effects; calculated geometries and energies; complete citations for Refs 38 and 39; and experimental and crystallographic details for the determination of absolute *dr*'s. See DOI: 10.1039/b000000x/

were catalysed by ionisable aluminium-containing Lewis acids such as Et_2AlCl .² Evans showed that the stereoselection arose through steric control. Chelation of the *N*-acyloxazolidinone **2** with AlEt_2^+ was suggested to produce the active dienophile, **3**, which is constrained to have a geometry in which the enone and the oxazolidinone ring lie within the same plane. Cycloaddition at the less-crowded face of **3**, opposite the *i*Pr group, leads to the major product.

We originally supposed that a similar mode of stereocontrol was present in our oxallyl-furan cycloadditions. Taking into account the *E* and *Z* isomers of **1**, there are four plausible transition-state geometries. These are shown in Scheme 4. The less-crowded geometries, **A** and **C**, were presumed to be preferred over the more-crowded **B** and **D**. Out of **A** and **C**, geometry **C** was thought to be preferred, since it would lead to the major product observed experimentally. Moreover, **C** has a suitable geometry for forming a chelate with ZnCl_2 , and the stereoselectivity was greater in the presence of ZnCl_2 .

However, the cycloadditions of **1_{Ph}** with substituted furans do not agree with this model. The reaction of **1_{Ph}** with 2-methylfuran afforded the same major product as furan itself (**I**), but the reaction of **1_{Ph}** with methyl 2-furoate provided the opposite diastereomer (**II**) as the sole cycloadduct.⁷ This reversal of stereoselectivity cannot easily be explained by the Evans-type mechanism.

We have undertaken a computational study, and report here that the factors that control stereoselectivity in oxallyl (4 + 3) cycloadditions are different from those established for Diels-Alder reactions involving the same oxazolidinone auxiliary. The cycloaddition of **1_{Ph}** with furan is found to involve only the *E* conformer – *i.e.* geometries **A** and **B** shown in Scheme 4. This is the case even in the presence of ZnCl_2 . The stereoselectivity is controlled not by steric repulsion between furan and the Ph group, but by “steric attraction”, where a stabilising CH- π interaction between furan and Ph favours cycloaddition at the more hindered π -face (geometry **B**). The sole involvement of **1-E**, and the presence or absence of attractive CH- π interactions at the TS, correctly predict the stereoselectivities for other oxazolidinones. The reversal of stereoselectivity observed with methyl 2-furoate is also explained by a mechanism involving only the *E* conformer of the oxallyl species.

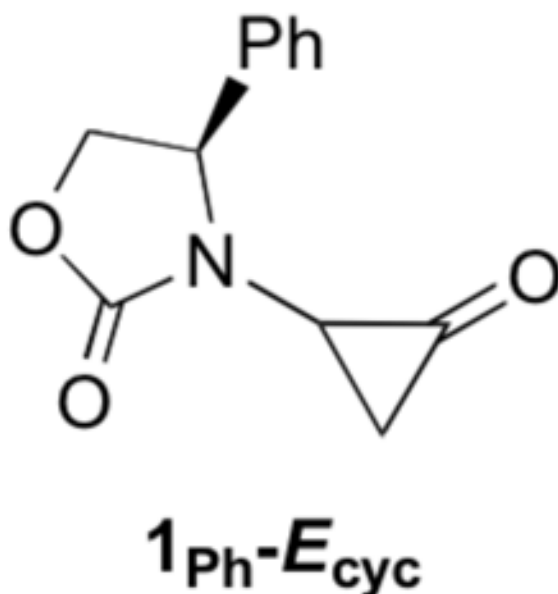
Results and discussion

Electronic structure of donor-substituted oxallyls

Density functional theory calculations were used to characterise the electronic structure of the oxazolidinone-substituted oxallyls **1**. The parent oxallyl, **4** (Fig. 1), is a diradical, but is not an energy minimum. Highly-correlated calculations and photoelectron spectroscopy show it to have an open-shell singlet ground state, which lies 1.3 kcal mol⁻¹ below the triplet and undergoes a barrierless ring closure to cyclopropanone.^{13,14} The diradical character of **4** is reflected quite well by B3LYP calculations.¹⁵⁻¹⁸ At the B3LYP/6-311G(2d,p) level, the singlet diradical of **4** lies 10.8 kcal mol⁻¹ below the closed-shell singlet (which has one imaginary vibrational frequency). Although a DFT treatment is not ideal for the singlet diradical, and it predicts the singlet diradical to lie 0.8 kcal mol⁻¹ above the triplet, this error is relatively small.

In the presence of a donor substituent, the closed-shell singlet of the oxallyl (zwitterion) is stabilised. For both **5a** (X = NMe₂) and **5b** (X = OMe), B3LYP/6-311G(2d,p) calculations indicate a closed-shell ground state, which is stable with respect to an open-shell representation. The sulfur-substituted analogue **5c** is more similar to **4** in retaining a singlet diradical ground state, but the closed-shell singlet lies only 2.9 kcal mol⁻¹ higher in energy.

The oxazolidinone-substituted oxyallyl **1_{Ph}** has electronic properties similar to **5a** and **5b**. B3LYP/6-311G(2d,p) calculations indicate a negligible singlet instability ($0.1 \text{ kcal mol}^{-1}$). The substituted structure, **1_{Ph}**, is a local minimum on the B3LYP/6-31G(d) potential energy surface, but attempts to locate **1_{Ph}-Z** led instead to the corresponding cyclopropanone. The cyclopropanone **1_{Ph}-E_{cyc}** is $4.8 \text{ kcal mol}^{-1}$ more stable than **1_{Ph}-E** (ΔH), and is the global minimum among all of the conformational and structural isomers of **1_{Ph}**. Details of these related species are given in the ESI.



The geometry of **1_{Ph}-E** is shown in Fig. 2. The CC bond lengths in **1_{Ph}-E** are similar to those in **5a** (also shown), and indicate that there is substantial electron delocalisation from nitrogen onto the allyl cation. The C_{α} - C_{β} distance (1.46 \AA) is 0.04 \AA shorter than the $C_{C=O}$ - $C_{C=C}$ bond in methyl vinyl ketone (**6**). The C_{β} - C_{ω} distance (1.40 \AA) is only 0.02 \AA longer than the C=C bond of acetone enolate (**7**). The C_{α} -N bond (1.33 \AA) is intermediate in length between a C-N and a C=N bond.

Fig. 2 also shows diagrams of the HOMO and LUMO of **1_{Ph}-E**.¹⁹ The HOMO is enolate-like, and has a larger coefficient on C_{ω} than on C_{α} . The LUMO has both allyl cation and iminium π^* character, with a larger coefficient on C_{α} than C_{ω} . All of these features indicate that **1_{Ph}-E** is best regarded as an iminium enolate.

Transition states for (4 + 3) cycloadditions

Detailed earlier studies by Cramer²⁰ have revealed that the cycloadditions of oxyallyl cations with dienes can take place by several different mechanisms. For example, the highly electrophilic 2-hydroxyallyl cation was calculated to undergo (4 + 3) cycloaddition with furan by a two-step process. In comparison, the combination of enolate and iminium character in **1_{Ph}** results in behaviour that is less markedly electrophilic. Transition states for the *endo* (4 + 3) cycloaddition of **1_{Ph}** with furan are depicted in Fig. 3. The reaction is a concerted process, and bond development at the TS is more advanced at the nucleophilic carbon, C_{ω} .

Although only the *E* isomer was located as an energy minimum for **1_{Ph}**, cycloaddition transition states can be located for either the *E* or *Z* geometry. The latter are substantially

higher in energy.²¹ For the *E* geometry, two concerted transition states were found—**TSA** and **TSB**—which lead to cycloadducts **II** and **I**, respectively. For the *Z* geometry, a concerted TS was located when furan adds to the more crowded π -face (**TSD**), but addition to the less crowded face is a stepwise process (**TSC**). Both **TSC** and **TSD** lie at high energies, due to electrostatic repulsion between the oxyallyl and carbonyl oxygens.

The *Z* transition states (**C** and **D**) are ≥ 14 kcal mol⁻¹ higher in energy than the *E* transition states (**A** and **B**); hence, cycloaddition takes place exclusively via **1_{Ph}-E**. Unexpectedly, however, it is 0.2 kcal mol⁻¹ easier ($\Delta\Delta H^\ddagger$) for furan to add to the *more* crowded face of **1_{Ph}-E** (**TSB**) than to the less crowded face (**TSA**). The corresponding free energy difference is similar, $\Delta\Delta G^\ddagger = 0.3$ kcal mol⁻¹. The small energy difference between **TSA** and **TSB** is in good qualitative agreement with the experimental stereoselectivity of 82:18 in favour of **I**.

Surprisingly, similar observations are made for the ZnCl₂-mediated cycloadditions of **1_{Ph}**.²² Unlike Evans' dienophile–AlEt₂⁺ complex, the ZnCl₂ complex of **1_{Ph}** is 6.2 kcal mol⁻¹ more stable as the monodentate form, **1_{Ph}-E·ZnCl₂** (Scheme 5), than as the chelate **1_{Ph}-Z·ZnCl₂**.²³ The cycloaddition transition structures for **1_{Ph}-E·ZnCl₂** and **1_{Ph}-Z·ZnCl₂** are analogous to those for uncomplexed **1_{Ph}**, except more asynchronous (see ESI). Coordination to ZnCl₂ lowers the activation energies by as much as 18.8 kcal mol⁻¹, but the exclusive participation of the *E* geometry is maintained. TSs for **1_{Ph}-Z·ZnCl₂** lie ≥ 4.2 kcal mol⁻¹ above those for **1_{Ph}-E·ZnCl₂**. Cycloaddition at the more crowded face is again preferred in **1_{Ph}-E·ZnCl₂**, the selectivity being $\Delta\Delta H^\ddagger = 1.1$ kcal mol⁻¹. This value is 0.9 kcal mol⁻¹ greater than in the thermal reaction, consistent with the higher experimental

Despite their quite different surface areas and dipole moments, the structures and energies of **TSA** and **TSB** are affected little by solvation, as modeled by CPCM calculations.²⁴ Free energies of solvation for **TSA** and **TSB** with B3LYP and several basis sets, and with additional solution-phase structure optimisations. The stereoselectivities for the thermal reactions in solution ranged from 0 to -0.4 kcal mol⁻¹ ($\Delta\Delta G^\ddagger$), compared with -0.3 kcal mol⁻¹ in the gas phase. Details are provided in the ESI.

The low energy of **TSB** appears to arise from an attractive interaction between furan and Ph. These two groups are suitably arranged for an edge-to-face CH– π interaction, with H-3 on the furan lying approximately 2.85 Å from the centre of the Ph ring. The interaction includes an electrostatic component, as indicated by a slightly (0.02e) more positive Mulliken charge on H-3 in **TSB** than in **TSA**, and is expected to include a dispersion component as in other aryl-aryl interactions.

Because the B3LYP functional does not generally model dispersion energies accurately,²⁵ we employed several other methods to quantify the role of dispersion in **TSA/B**. Grimme's simple empirical formula (B3LYP-D, 2006), which sums the interatomic interactions in a pairwise fashion,²⁶ predicts that the total dispersion energy, E_{disp} , is 2.7 kcal mol⁻¹ larger (more stabilizing) in **TSB** than in **TSA**. The furan–Ph interaction is 4.3 kcal mol⁻¹ larger in **TSB** than in **TSA**.

The B3LYP-D dispersion correction strongly favours **TSB**, and indeed overestimates the stereoselectivity.²⁷ Grimme's B97-D functional,²⁸ which is explicitly parameterised to provide a more sophisticated treatment of short- and long-range interactions, with the aug-cc-pVTZ basis set indicates a 2.2 kcal mol⁻¹ preference for **TSB**. A similar result is obtained with Truhlar's M06-2X functional,²⁹ which includes attractive terms mimicking dispersion. The π -facial discrimination between **TSA** and **TSB** at the M06-2X/6-31G(d) level is $\Delta\Delta E^\ddagger = 1.4$ kcal mol⁻¹, and this value increases to 2.2 kcal mol⁻¹ upon full geometry optimisation. Although these newer functionals have not been as extensively benchmarked for cycloaddition transition states as B3LYP, and indeed overestimate the

stereoselectivity, they are consistent in their support for a stabilising CH– π interaction in **TSB**.

Stereoselectivities for other oxazolidinones

A combination of steric repulsion and attractive CH– π interactions determines the stereoselectivity induced by other oxazolidinones. We calculated transition states analogous to **TSA** and **TSB** for 4-Bn- and 4-*i*Pr-5,5-Ph₂-substituted oxazolidinones, and determined their experimental *dr*'s.³⁰ The predicted and observed selectivities are listed in Table 1.

When the 4-phenyl substituent on the oxazolidinone is replaced by a benzyl group, the possibility of a stabilising CH– π interaction is eliminated and replaced by a repulsive furan–alkyl interaction. This is illustrated in Fig. 4. The opposite stereoisomer is now favoured by 0.1 kcal mol⁻¹. Experimentally, **II** is indeed obtained as the major product, with a *dr* of 23:77 (**I:II**). An even higher selectivity in favour of **II** is obtained with the 4-*i*Pr-5,5-Ph₂-oxazolidinone. In this case, the favoured TS benefits from both the minimisation of repulsive interactions between furan and the *i*Pr group, and a stabilising CH– π interaction between furan and the C-5 Ph group *trans* to *i*Pr. The calculated selectivity of 2.3 kcal mol⁻¹ in favour of **II** agrees with the higher experimental selectivity for **II** (*dr* 6:94). In the absence of the two phenyl rings at C-5, the diastereoselectivity is only 45:55.⁶ These correlations accentuate the powerful impact that a non-bonding force such as CH– π interaction can exert on the stereochemical course of cycloadditions.

Reversal of stereoselectivity for methyl 2-furoate

The *E*-only mechanism predicts that the cycloadditions of **1_{Ph}** with furan and methyl 2-furoate should give opposite stereoselectivities. The four stereo- and regioisomeric TSs for cycloaddition of **1_{Ph}-E** with methyl 2-furoate are shown in Fig. 5. The TS leading to the experimental major product, *syn*-**II** (**TSE**), lies ≥ 1.9 kcal mol⁻¹ below the other three TSs. The *syn* regioselectivity is expected, as it is favoured by the reactants' frontier orbital coefficients. The reversal of stereoselectivity can be ascribed to repulsive interactions between the Ph group and the 2-COOMe group. In **TSG**, H-3 on the furan lies only 0.05 Å further from the midpoint of the Ph ring than in **TSB**, but the electrostatic repulsion between the Ph π cloud and the carbonyl group at C-2 of the furan outweighs the stabilising effect of CH– π attraction. Cycloaddition therefore takes place preferentially through the less crowded *syn* TS.

Conclusions

Density functional theory calculations make it clear that only the *E* isomer of the oxyallyl **1** undergoes cycloaddition with furans. The *Z* isomer is subject to severe electrostatic repulsion between the oxyallyl and carbonyl oxygen atoms, and this destabilisation is not overcome even upon coordination to ZnCl₂. Santos et al. have recently reported related calculations on Evans' Diels–Alder reactions (Scheme 2), and suggest that rather than taking place via the chelate, these reactions instead involve a complex of **2** in which the carbonyl groups are antiparallel (*i.e.* *E*), and each is bound to an AlEt₂Cl.³¹ They proposed that the stereoselectivity can then be traced to repulsive interactions between the Et groups on the Lewis acid and the *i*Pr group on the oxazolidinone. Antiparallel conformations of *N*-acyloxazolidinones have also been invoked in oxazolidinone-directed nitrile ylide cycloadditions⁵ and dynamic kinetic resolutions of α -haloketones.³² Santos' calculations confirmed, however, that Evans' original sterically-controlled mechanism of stereoselection would still be valid within a stoichiometric regime where the chelate would exist.³¹

The origin of stereinduction in the (4 + 3) cycloadditions of **1_{ph}** is quite distinct from these processes, and could be relevant to various other asymmetric reactions. CH– π interactions are well known to influence conformational equilibria, crystal packing, the structures of biological molecules, and molecular recognition.^{33,34} Previous computational studies have shown that CH– π interactions are responsible for the *endo* selectivity of the Diels–Alder reaction of butadiene with cyclopropene³⁵ and the hetero-Diels–Alder reactions of *ortho*-xylylenes with benzaldehyde.³⁶ The calculated selectivities in these cases amounted to 1–2 kcal mol⁻¹.

CH– π interactions appear to be general design elements in asymmetric reactions. We recently discovered a similar example of this form of stereocontrol, in (4 + 3) cycloadditions of α -methylbenzyloxy-substituted siloxyallyl cations.³⁷ Like **1_{ph}**, these oxyallyl cations are relatively rigid species, and the aromatic group is held roughly perpendicular to the molecular plane. Furan was found to add to the aryl-containing face with a selectivity of approximately 1 kcal mol⁻¹. It is likely that further examples of stereocontrol via CH– π interactions will be reported in the future.

Experimental

Density functional theory were performed using the Gaussian 03³⁸ and Gaussian 09³⁹ packages. The nature of each stationary point was checked by means of frequency calculations, and transition states were further verified by IRC calculations.⁴⁰ Zero-point energy and thermal corrections were derived from the B3LYP or M06-2X frequencies, but not scaled. The effects of solvation were simulated by means of CPCM calculations²⁴ using UAKS radii (Gaussian 03).

Acknowledgments

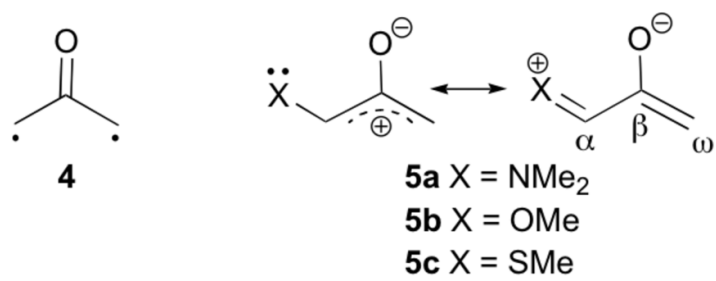
We thank the NIH, NSF, and Australian–American Fulbright Commission for generous financial support, and the NCSA, UCLA ATS, and UCLA IDRE for computer resources.

Notes and references

1. Evans DA. *Aldrichim Acta*. 1982; 15:23. Zappia G, Cancelliere G, Gacs-Baitz E, Delle Monache G, Misiti D, Nevola L, Botta B. *Current Org Synth*. 2007; 4:238. Ager DJ, Prakash I, Schaad DR. *Aldrichim Acta*. 1997; 30:3. Evans, DA.; Helmchen, G.; Rüping, M. *Asymmetric Synthesis – The Essentials*. 2. Christmann, M.; Bräse, S., editors. Wiley-VCH; Weinheim: 2008. p. 3-9.
2. Evans DA, Chapman KT, Bisaha J. *J Am Chem Soc*. 1984; 106:4261. Evans DA, Chapman KT, Bisaha J. *Tetrahedron Lett*. 1984; 25:4071. Evans DA, Chapman KT, Hung DT, Kawaguchi AT. *Angew Chem, Int Ed Engl*. 1987; 26:1184. Evans DA, Chapman KT, Bisaha J. *J Am Chem Soc*. 1988; 110:1238.
3. Banks MR, Blake AJ, Cadogan JIG, Doyle AA, Gosney I, Hodgson PKG, Thorburn P. *Tetrahedron*. 1996; 52:4079.
4. Evans DA, Brown Ripin DH, Johnson JS, Shaughnessy EA. *Angew Chem Int Ed Engl*. 1997; 36:2119.
5. Sibi MP, Soeta T, Jasperse CP. *Org Lett*. 2009; 11:5366. [PubMed: 19877629]
6. Xiong H, Hsung RP, Berry CR, Rameshkumar C. *J Am Chem Soc*. 2001; 123:7174. [PubMed: 11459504]
7. Antoline JE, Hsung RP. *Synlett*. 2008:739.
8. Hartung IV, Hoffmann HMR. *Angew Chem Int Ed*. 2004; 43:1934.
9. Harmata M. *Acc Chem Res*. 2001; 34:595. [PubMed: 11456477]
10. Stark CBW, Pierau S, Wartchow R, Hoffmann HMR. *Chem Eur J*. 2000; 6:684.
11. MaGee DI, Godineau E, Thornton PD, Walters MA, Sponholtz DJ. *Eur J Org Chem*. 2006:3667.

12. We use the term “endo” to denote the relationship between the diene and the oxyallyl oxygen in **I** and the TSs leading to them. Hoffmann has used the term “compact” to describe this type of (4 + 3) cycloaddition geometry: see Hoffmann HMR. *Angew Chem internat Edit.* 1973; 12:819.
13. Coolidge MB, Yamashita K, Morokuma K, Borden WT. *J Am Chem Soc.* 1990; 112:1751.
14. Ichino T, Villano SM, Gianola AJ, Goebbert DJ, Velarde L, Sanov A, Blanksby SJ, Zhou X, Hrovat DA, Borden WT, Lineberger WC. *Angew Chem Int Ed.* 2009; 48:8381.
15. Becke AD. *J Chem Phys.* 1993; 98:5648.
16. Stephens PJ, Devlin FJ, Chablowski CF, Frisch MJ. *J Phys Chem.* 1994; 98:11623.
17. Lee C, Yang W, Parr RG. *Phys Rev B.* 1988; 37:785.
18. The singlet diradical was approximated by use of the guess=mix keyword in Gaussian 03 (Ref. 38).
19. Orbitals were calculated at the HF/6-31G//B3LYP/6-31G(d) level.
20. Cramer CJ, Barrows SE. *J Org Chem.* 1998; 63:5523. Cramer CJ, Barrows SE. *J Phys Org Chem.* 2000; 13:176.
21. Activation energies were calculated with respect to the most stable isomer **1Ph-E_{cyc}**.
22. The LANL2DZ basis set and ECP were used for Zn: Wadt WR, Hay PJ. *J Chem Phys.* 1985; 82:284.
23. At the B3LYP/6-31G(d) level, the AlMe₂⁺ chelate of the Me analogue of **3** (where *i*Pr is replaced by Me) is 24 kcal mol⁻¹ more stable than the corresponding monodentate complex with *anti* (*i.e.* *E*) carbonyls where Al is bound to the oxyallyl oxygen.
24. Barone V, Cossi M. *J Phys Chem A.* 1998; 102:1995. Barone V, Cossi M, Tomasi J. *J Comput Chem.* 1998; 19:404.
25. Allen MJ, Tozer DJ. *J Chem Phys.* 2002; 117:11113. Zimmerli U, Parrinello UM, Koumoutsakos PJ. *J Chem Phys.* 2004; 120:2693. [PubMed: 15268413] Cerny J, Hobza P. *Phys Chem Chem Phys.* 2005; 7:1624. [PubMed: 19787917]
26. Grimme S. *J Comput Chem.* 2004; 25:1463. [PubMed: 15224390] Grimme S. *J Comput Chem.* 2006; 27:1787. [PubMed: 16955487]
27. Grimme²⁶ recommends the use of polarised triple-zeta AO basis sets as a minimum for DFT-D calculations. The value of $\Delta\Delta E^\ddagger(\text{TSA}-\text{TSB})$ obtained with the 6-31G(d) basis set (3.0 kcal mol⁻¹) is very similar to the value obtained when the electronic energies are calculated with the 6-311G(2d,p) basis at the same geometries (3.1 kcal mol⁻¹).
28. Antony J, Grimme S. *Phys Chem Chem Phys.* 2006; 8:5287. [PubMed: 19810407]
29. Zhao Y, Truhlar DG. *Acc Chem Res.* 2008; 41:157. [PubMed: 18186612] Zhao Y, Truhlar DG. *Theor Chem Account.* 2008; 120:215.
30. Note: In the original report (Ref. 6), the absolute stereochemistry of the major and minor products obtained using the 4-Bn- and 4-*i*Pr-5,5-Ph₂-oxazolidinone auxiliaries were assumed to be the same as those obtained with 4-Ph-oxazolidinone (the latter having been determined by X-ray crystallography). Our present DFT predictions, however, prompted us to determine the absolute stereochemistries for these two auxiliaries. Following the (4 + 3) cycloadditions, reduction of the cycloheptenone carbonyl group and acylation of the resulting alcohols afforded nitrobenzoates, which were characterised by X-ray crystallography. The absolute stereoselectivities in both cases were found to be opposite from those originally supposed. Details are provided in the ESI.
31. Bakalova SM, Duarte FJS, Georgieva MK, Cabrita EJ, Santos AG. *Chem Eur J.* 2009; 15:7665.
32. Santos AG, Candeias SX, Afonso CAM, Jenkins K, Caddick S, Treweeke NR, Pardoe D. *Tetrahedron.* 2001; 57:6607. Santos AG, Pereira J, Afonso CAM, Frenking G. *Chem Eur J.* 2005; 11:330.
33. Nishio, M.; Hirota, M.; Umezawa, Y. *The CH/π Interaction: Evidence, Nature, and Consequences.* Wiley-VCH; New York: 1998. Nishio M, Umezawa Y, Hirota M, Takeuchi Y. *Tetrahedron.* 1995; 51:8665. Nishio M. *Tetrahedron.* 2005; 61:6923.
34. Gillard RE, Raymo FM, Stoddart JF. *Chem Eur J.* 1997; 3:1933.
35. Sodupe M, Rios R, Branchadell V, Nicholas T, Oliva A, Dannenberg JJ. *J Am Chem Soc.* 1997; 119:4232.
36. Ujaque G, Lee PS, Houk KN, Hentemann MF, Danishefsky SJ. *Chem Eur J.* 2002; 8:3423.
37. Krenske EH, Houk KN, Harmata M. *Org Lett.* 2010; 12:444. [PubMed: 20063884]

38. Frisch, MJ., et al. Gaussian 03, Revision C.02. Gaussian, Inc; Wallingford, CT: 2004.
39. Frisch, MJ., et al. Gaussian 09, Revision A.02. Gaussian, Inc; Wallingford, CT: 2009.
40. Gonzalez C, Schlegel HB. J Chem Phys. 1989; 90:2154. Gonzalez C, Schlegel HB. J Chem Phys. 1990; 94:5523.



	closed-shell singlet	open-shell singlet	triplet
4	11.0	0.8	0
5a	0	–	19.4
5b	0	–	10.5
5c	2.9	0	6.7

Fig. 1. Energies of different electronic states of oxyallyls **4** and **5a–c** [ΔE , kcal mol⁻¹, B3LYP/6-311G(2d,p)].

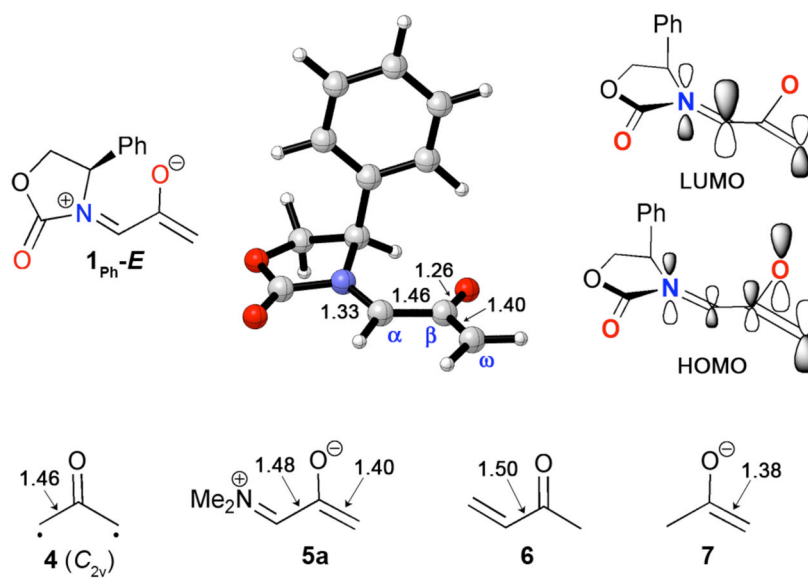


Fig. 2. Structure and molecular orbitals of 1_{Ph}-E , and related compounds [bond lengths in Å, B3LYP/6-31G(d)].

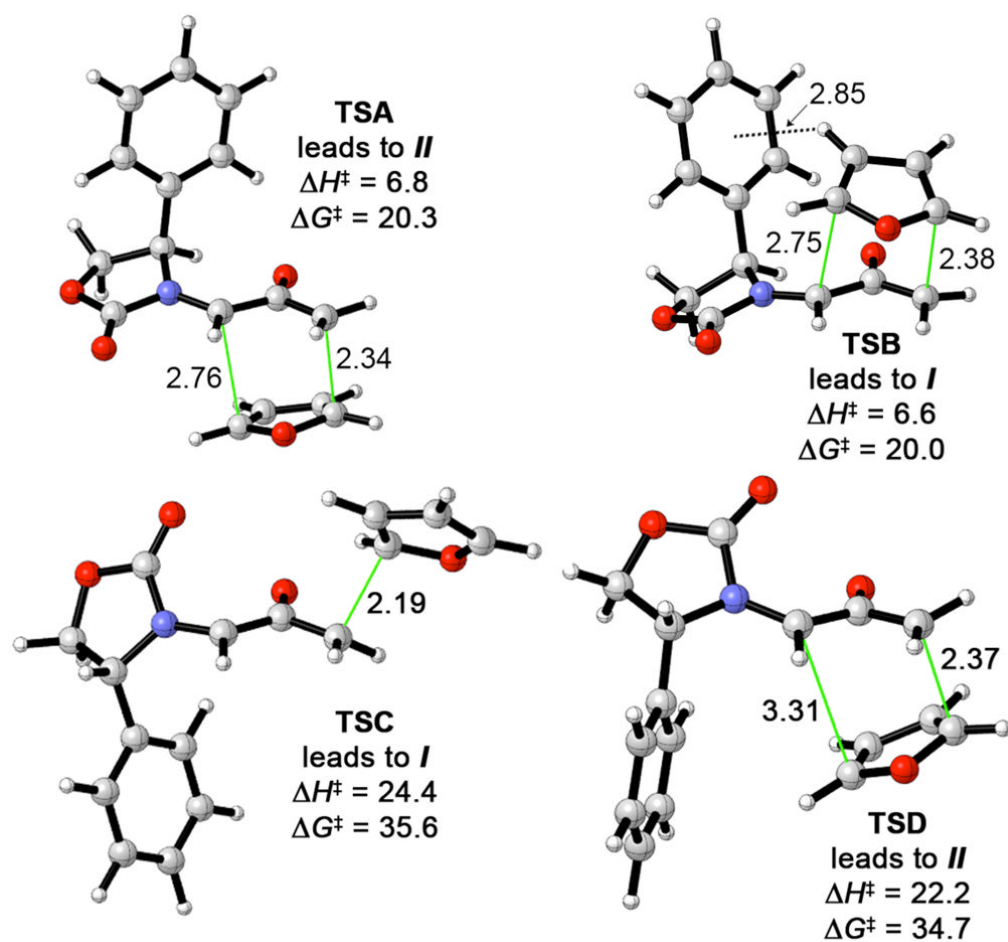


Fig. 3. Transition structures and activation energies for the cycloaddition of **1Ph** with furan [298.15 K, B3LYP/6-31G(d)].

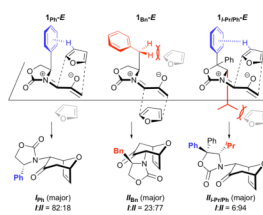


Fig. 4. Control of stereoselectivity by a combination of stabilising furan–Ph interactions and destabilising furan–alkyl interactions for **1_{Ph}**, **1_{Bn}**, and **1_{*i*-Pr/Ph}**. Note: For **1_{*i*-Pr/Ph}**, C-4 of the oxazolidinone has the *S* configuration, whereas **1_{Ph}** and **1_{Bn}** are *R*.

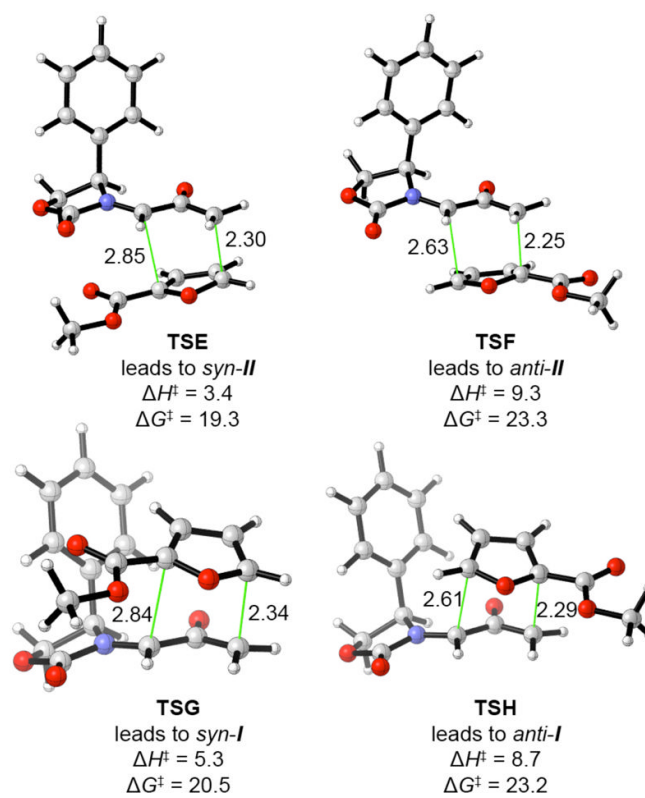
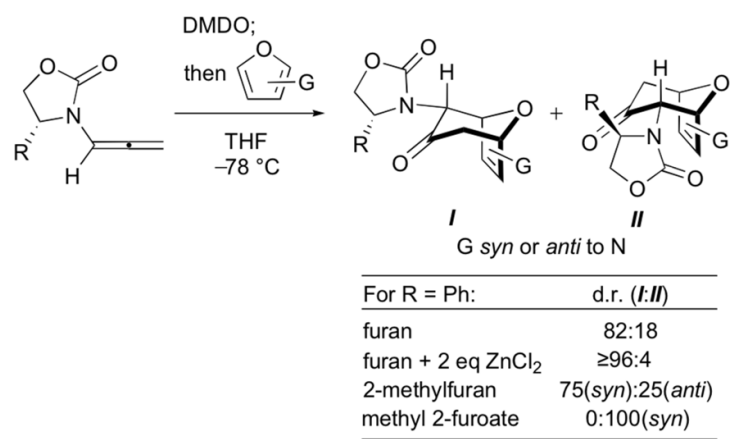
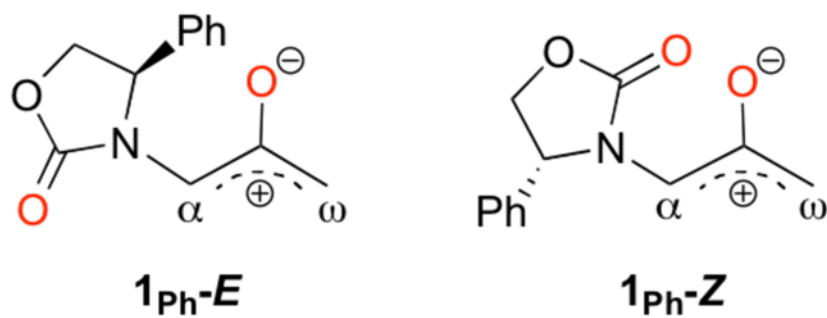


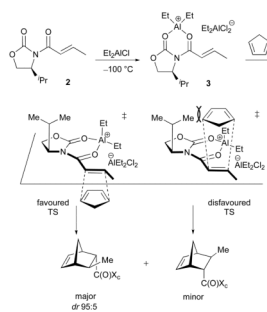
Fig. 5. Transition structures and activation energies for the cycloaddition of **1Ph** with methyl 2-furoate [298.15 K, B3LYP/6-31G(d)].



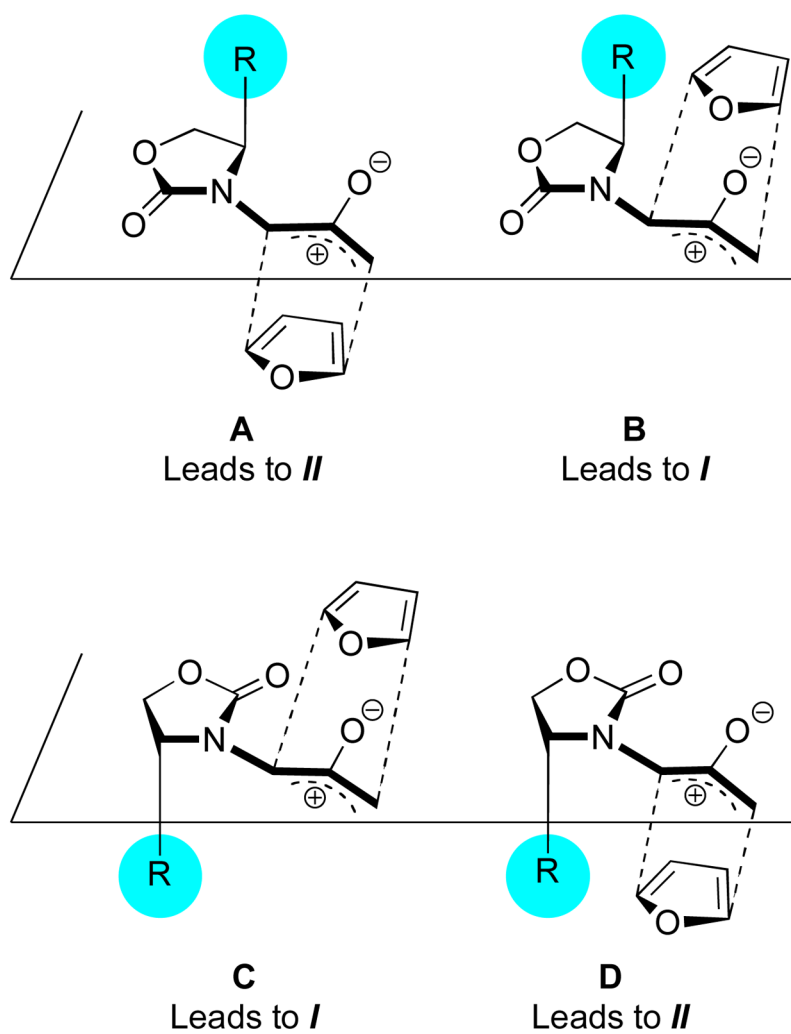
Scheme 1.
Oxazolidinone-directed asymmetric (4 + 3) cycloadditions of oxyallyls with furans.



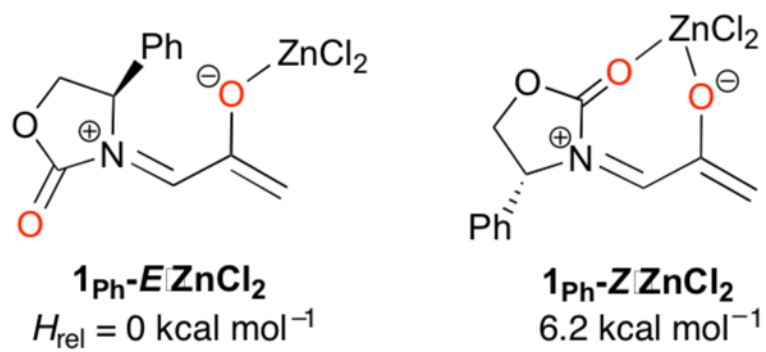
Scheme 2.
Isomers of the oxyallyl **1_{Ph}**.



Scheme 3.
Evans' oxazolidinone-directed asymmetric Diels–Alder reactions.



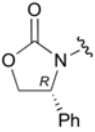
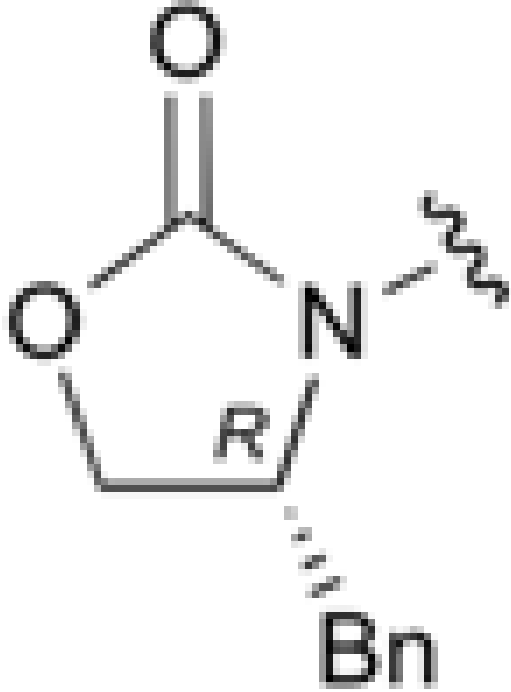
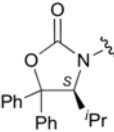
Scheme 4.



Scheme 5.

Table 1

Calculated and experimental stereoselectivities for (4 + 3) cycloadditions of oxazolidinone-substituted oxyallyls with furan

Oxazolidinone	Calcd $\Delta\Delta H^\ddagger$ (TSA-TSB) ^b	Exptal <i>dr</i> (<i>I:II</i>) ^a
	0.2	82:18
	-0.1	23:77
	-2.3	6:94

^a 298.15 K, kcal mol⁻¹, B3LYP/6-31G(d).

^b THF, -40 to -50 °C.